Single Crystal Ni_5Zn_{21} Nanowire Arrays Fabricated by Electrodeposition in Anodic Alumina Membranes

Chong Jia, Weifeng Liu, Bei Zhang, Chuangui Jin, Lianzeng Yao, Weili Cai,* and Xiaoguang Li
Department of Materials Science and Engineering, University of Science and Technology of China, Hefei 230026, P. R. China

(Received October 18, 2004; CL-041230)

Large-area, high-filling rate, uniform, and single-crystal Ni_5Zn_{21} nanowire arrays have successfully been synthesized by dc electrodeposition into the nanochannels of anodic alumina membranes (AAM).

Nanowires have been a focus of much attention for their interesting properties and wide-range potential applications in nanodevices for several years.[1,2] Among various synthetic techniques, electrochemical deposition synthesis into nanochannels of the AAM has been proved to be a versatile, simple method for preparation of nanowires. Many metals[3,4] and semiconductors[5,6] have been synthesized in this way. But, fabrications of metal alloy nanowires are still a challenge. Alloys usually have some properties better than the corresponding pure metals. For example, Sn–Pb alloy has a lower melting point than Sn and Pb, Fe–Co alloy is a more effective magnetic material than the pure Fe or Co, and Cu–Ni alloy possesses better thermoelectricity. Ni–Zn is known to have a highly improved degree of the corrosion resistance in comparison with the pure zinc,[7] besides, it is the matrix of the Raney-type structure,[8] an excellent electrocatalyst. However, studies of the Zn–Ni alloy have almost been concentrated on its films before. In this letter, large-area, high-filling rate, uniform, and single-crystal Ni_5Zn_{21} nanowire arrays have successfully been synthesized by dc electrodeposition into the nanochannels of AAM.

The AAM used in this work was prepared via a two-step anodic oxidation process of aluminum (purity: 99.999%) in a 0.3 M $H_2C_2O_4$ solution, which was similar to that described previously.[9] After anodization, the central substrate was removed by 1 M $CuCl_2$ solution, and the surrounding aluminum was retained as a support. Then, the barrier layer was dissolved in 5 wt % H_3PO_4 solution at 30 °C for 1 h. Finally, a Au layer was sputtered onto one side of the through-hole AAM to serve as the working electrode. Electrodeposition was carried out in a common two-electrode electrochemical cell using a graphite plate as the counter electrode. The electrolyte solution consisted of 50 g/L $NiSO_4 \cdot 7H_2O$, 30 g/L $ZnCl_2$, 100 g/L NH_4Cl, and 15 g/L H_3BO_3. Before electrodeposition, the AAM was immersed into the electrolyte solution and evacuated using a pump to get rid of bubbles in the nanochannels. Electrodeposition was performed at room temperature for 1 h under a constant current density of 2 mA/cm^2 which was strictly controlled by a potentiostat/galvanostat (HDV-7C). After electrodeposition, the back Au film was carefully scraped off using Al_2O_3 powders. Finally, the sample was rinsed with deionized water and dried in air for further analysis.

The crystal structure of the obtained Ni–Zn alloy nanowires was analyzed by X-ray diffraction (XRD) on an X-ray diffractometer (Rigaku, D/MAX-γA) with Cu Kα radiation (λ = 0.15418 nm). The morphology of the Ni–Zn alloy nanowires was observed on a transmission electron microscope (TEM, H-800) and a field emission scanning electron microscope (FE-SEM, JSM-6700F).

XRD patterns of the obtained nanowires are shown in Figure 1. Curve 1a is the XRD pattern for the as-prepared nanowire array. It can be seen that there is only a very sharp diffraction peak at $2\theta = 42.7°$ ($d = 0.211$ nm), which implies that all the Zn–Ni nanowires have the same orientation. Curve 1b is the XRD pattern for the sample after grinding. It is clear that more other peaks appear in the diffraction pattern due to random orientation of the nanowires, and all the peaks can be indexed to the cubic Ni_5Zn_{21} (JCPDS, 6-653), which indicates that the phase of Ni–Zn alloy nanowires is very pure.

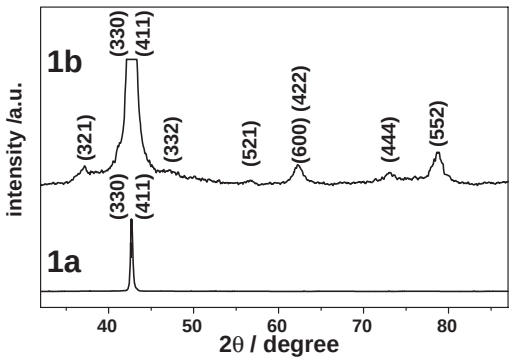

Figure 1. XRD patterns for Ni_5Zn_{21} nanowire arrays. (1a): as-obtained; (1b): after grinding.

Typical TEM images of the Ni_5Zn_{21} nanowires liberated from the AAM by immersing the AAM into 2 M NaOH solution for 1 h are displayed in Figure 2. The inset in Figure 2b is the corresponding electron diffraction (ED) pattern of a single nanowire. It can be seen from Figure 2 that these nanowires are straight with a uniform diameter of about 40 nm in agreement with the pore diameter of the AAM used, and the surfaces of the nanowires are very smooth. The diffraction spots in the ED pattern are identified to the (600), ($3\bar{3}0$), and (330) planes of the single crystal cubic Ni_5Zn_{21}, respectively, which is consistent with the XRD results.

Figure 3 presents typical FE-SEM images of the Ni_5Zn_{21} nanowire arrays after the AAM was partly etched off by 1 M NaOH. It is clear that almost every pore is filled with Ni_5Zn_{21} nanowires, and the surfaces of the nanowires are very smooth. The measured diameter of the Ni_5Zn_{21} nanowires is about 40 nm, which corresponds satisfactorily to the pore diameter of the AAM used. The Ni_5Zn_{21} nanowires with a high filling rate are very dense and have the same height in large area.

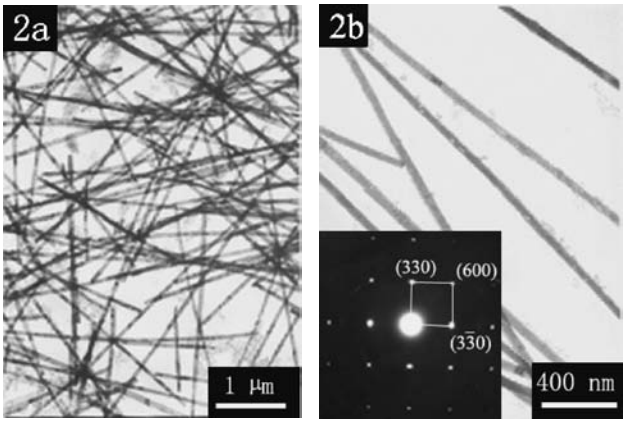

Figure 2. TEM images of Ni_5Zn_{21} nanowires liberated from the AAM by immersing it into 2 M NaOH solution for 1 h. The insert in Figure 2b is the corresponding ED pattern of a single nanowire.

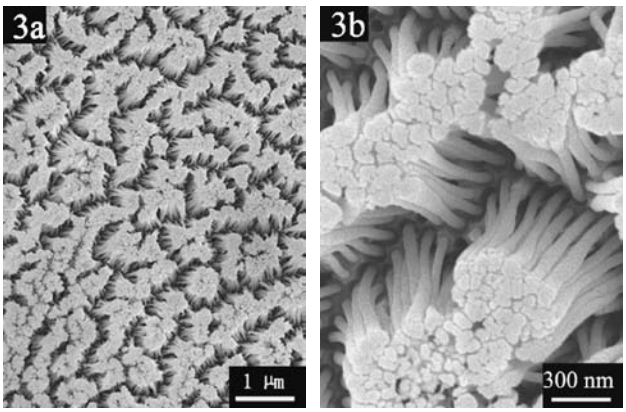

Figure 3. Typical SEM images of the Ni_5Zn_{21} nanowire arrays. (3a) Low magnification; (3b) High magnification.

For electrodeposition into the nanochannels of the AAM, Jin et al.[4] have discussed several key points that can greatly influence the synthesis of nanowires. Besides, the quality of the AAM and the composition of the electrolyte solution can also affect the quality and the components of the nanowires. Furthermore, many other factors, such as the current density,[10] the voltage,[11] and the temperature, are also essential to determine the structure and the component of the Zn–Ni alloy nanowires.

Generally speaking, electrodeposition of Zn–Ni results in an anomalous type of the Zn–Ni alloy,[12] since the less noble metallic zinc deposits preferentially and its percentage in the deposit is higher than that in the electrolyte. Many models have been proposed to explain this anomalous electrodeposition.[13–15] Dybkov[16] has suggested that the diffusion rate of Zn^{2+} is much higher than that of Ni^{2+} because of the difference in the melting points (Zn: 693 K, Ni: 1728 K) and the thermal expansion coefficients (Zn: $\alpha_{20} = 30.0 \times 10^{-6}\,K^{-1}$, Ni: $\alpha_{20} = 13.5 \times 10^{-6}\,K^{-1}$). Therefore, the hexagonal Ni_3Zn_{22} is formed more easily than the cubic Ni_5Zn_{21}. But, the one-dimensional nanochannels in our experiments restrict the diffusion of Zn^{2+} and Ni^{2+} so greatly that the ion concentrations in the electrolyte solution become a determinant factor. Under this condition, only the Ni_5Zn_{21} nanowires can be deposited using a current density ranging from 0.5 to 10 mA/cm^2. This result is very different from the electrodeposition of Zn–Ni alloy films.

It has been reported that the Zn–Ni alloys have a highly improved degree of the corrosion resistance in comparison with the pure zinc,[7] which is confirmed in the our TEM observations. For pure Zn nanowires, it takes about 5 to 10 min to liberate them from the AAM.[17] If the sample is immersed into 2 M NaOH solution for more than 20 min, the Zn nanowires will be completely dissolved. In contrast, it takes more than 30 min to separate the Ni_5Zn_{21} nanowires from the AAM, which indicates the Ni_5Zn_{21} nanowires are much denser than the Zn nanowires. Furthermore, after being immersed into 2 M NaOH solution for several hours, the Ni_5Zn_{21} nanowires still can be seen in the TEM observations (as shown in Figure 2), which indicates that the corrosion resistance of the Ni_5Zn_{21} nanowires has been greatly improved.

This work is supported by the National Natural Science Foundation of China under Grant No. 50128202.

References

1 A. M. Morales and C. M. Lieber, *Science*, **279**, 208 (1998).
2 X. F. Duan, Y. Huang, Y. Cui, J. F. Wang, and C. M. Lieber, *Nature*, **409**, 66 (2001).
3 C. G. Jin, G. W. Jiang, W. F. Liu, W. L. Cai, L. Z. Yao, Z. Yao, and X. G. Li, *J. Mater. Chem.*, **13**, 1743 (2003).
4 C. G. Jin, W. F. Liu, C. Jia, X. Q. Xiang, W. L. Cai, L. Z. Yao, and X. G. Li, *J. Cryst. Growth*, **258**, 337 (2003).
5 C. G. Jin, X. Q. Xiang, C. Jia, W. F. Liu, W. L. Cai, L. Z. Yao, and X. G. Li, *J. Phys. Chem. B*, **108**, 1844 (2004).
6 Y. W. Wang, L. D. Zhang, C. H. Liang, G. Z. Wang, and X. S. Peng, *Chem. Phys. Lett.*, **357**, 314 (2002).
7 A. Abibsi, N. R. Short, and J. K. Dennis, *Trans. Inst. Met. Finish.*, **69**, 45 (1991).
8 E. Endoh, H. Otouma, T. Morimito, and Y. Oda, *Int. J. Hydrogen Energy*, **12**, 473 (1987).
9 H. Masuda, H. Yamada, M. Satoh, and H. Asoh, *Appl. Phys. Lett.*, **71**, 2770 (1997).
10 I. Brooks and U. Erb, *Scr. Mater.*, **44**, 853 (2001).
11 Z. Y. Zhou and T. J. O'Keefe, *Surf. Coat. Technol.*, **96**, 191 (1997).
12 G. Roventi, R. Fratesi, R. A. Della Guardia, and G. Barucca, *J. Appl. Electrochem.*, **30**, 173 (2000).
13 D. E. Hall, *Plat. Surf. Finish.*, **70**, 47 (1983).
14 M. J. Nicol and H. I. Philip, *J. Electroanal. Chem.*, **70**, 233 (1976).
15 V. G. Roev and N. V. Gudin, *Elektrokhimiya*, **31**, 532 (1995).
16 V. I. Dybkov, *Powder Metall. Met. Ceram.*, **40**, 426 (2001).
17 C. Jia, W. F. Liu, C. G. Jin, B. Zhang, L. Z. Yao, W. L. Cai, and X. G. Li, *Chem. Lett.*, **33**, 634 (2004).

Published on the web (Advance View) November 27, 2004; DOI 10.1246/cl.2005.20